Iraqi Journal of Industrial Research, Vol. 11, No. 2 (2024)

Iraqi Journal of Industrial Research (IJOIR)

Journal homepage: http://ijoir.gov.iq

Investigating the Electrical, Power Factor, and Figure of Merit Characteristics of Cadmium Oxide Nanostructures Fabricated via Thermal Evaporation in Vacuum

[1]**Wafaa Khalid Khalef***, [1]**Rafah Alwan Nassif**, [1]**Raghad Hamid Hilal**, [2]**Sura R. Mohammed**

[1]Department of Applied Science, University of Technology, Iraq

[2]Ministry of Science and Technology, Iraq

Article information

Article history:
Received: November, 13, 2023
Accepted: February, 09, 2024
Available online: October, 20, 2024

Keywords:
Cadmium oxide nanostructure,
Oblique angle deposition (OAD),
Oblique deposition

Corresponding Author:
Wafaa Khalid Khalef
drwafaa1980@gmail.com

DOI:
https://doi.org/10.53523/ijoirVol11I2ID408

Abstract

A cadmium dioxide nanostructure was fabricated on silicon and quartz substrates through oblique angle deposition (OAD). The synthesis involved the initial thermal evaporation of high-purity cadmium metal films at varying deposition angles on the substrates, followed by a 1.5-hour oxidation process at 773 K in a conventional furnace to produce cadmium oxide nanostructures. X-ray diffraction (XRD) analysis revealed the development of crystalline structures within the cadmium oxide (CdO) films. The deposition angle exhibited a significant impact, influencing the preferred orientation along the (111) planes more substantially than the normal incident angle. I-V measurements and assessments of electrical conductivity were conducted under both light and dark conditions for the CdO films. The photocurrent generated in an oblique (Al/CdO/p-Si/Al) heterojunction exceeded that of a standard detector under illumination. The investigation explored the thermoelectric properties of CdO nanomaterials, including the figure of merit (M), power factor (P.F.), and Seebeck coefficient (S), for both normally deposited and obliquely deposited films. The results demonstrated an enhancement in the figure of merit with oblique deposition, potentially attributed to increased roughness, resulting in reduced thermal conductivity and an elevated figure of merit. All findings indicated superior performance for deposition angles (θº = 50º & 70º) in comparison to normal deposition (θº = 0º).

1. Introduction

Many researchers have focused on cadmium oxide (CdO) due to its applications, specifically in the field of optoelectronic devices such as solar cells [1, 2] phototransistors and diodes, transparent electrodes, gas sensors [3, 4] CdO is an n-type semiconductor with a rock-salt crystal structure (F.C.C) and possesses a direct band gap of (2.2-2.5) eV [5]. Various techniques have been employed to prepare CdO thin films such as spray pyrolysis [6] sputtering [7, 8] solution growth [9] activated reactive evaporation [10] pulsed laser sputtering [11] and sol-gel method [12]. The glancing angle deposition (GLAD) technique is the extension of the commonly used oblique angle deposition (OAD) in the thin film deposition community which has been practiced for many years [13]. In the state of obliquely deposited thin films, it is noticed forms like high-density rods or needles, are separated by low-density voids [14]. Then the film density is less than the material density in its bulk and the film density decreases with increasing deposition angle (θ˚) [15]. The oblique deposition produces columnar structures due to the shadowing effect and random fluctuations during film growth [16].

Longer Nanorods develop more quickly due to the shadowing effect, which lowers the number density of Nanorods. Large clusters of slanted rods interspersed with smaller and shorter rods are common topologies created as a result of the fluctuations in the deposition fluxing (unstable deposition rates or angular distributions of the incoming particles) which further complicate the creation of uniform nanostructures [17]. The purpose of this work is to investigate how the deposition angle θ° affects the optical characteristics of CdO films made from cadmium thin films that have been thermally evaporated both obliquely and normally.

2. Experimental Procedure

On a glass substrate, cadmium thin films were normally and obliquely formed by thermal evaporation of the Thermionic Laboratory Inc. German Production Company type at various angles θ = (0°, 50°, and 70°). The (Cd) material was put in a vacuum chamber at a pressure of (7x10-5) Torr, within a tungsten (W) boat. For all samples, the distance between the source and substrate was maintained at 15 cm in order to achieve a consistent and homogenous film thickness over a sizable area. The glass ware substrate (2 cm x 2 cm) had a 15-minute ultrasonic treatment (Transistor/UL Transonic T-7) with acetone and ethanol. Following this, they were rinsed with deionized water and dried with nitrogen gas. Ultimately, the slides were dried at 150C˚ using a magnetic stirrer and a piece of hot plate equipment. To create cadmium oxide, each sample was annealed for 1:5 hours at a temperature of 773 K in a furnace of the KSL-1100X type. The average grain size (D) of the polycrystalline cadmium oxide films can be calculated from the (X – ray) spectrum by means of Full Width at Half Maximum (FWHM) method (Scherer relation) [18]:

$$D = \frac{A\,\lambda}{\beta \cos\theta} \qquad (1)$$

Where (β) is the full width at half maximum of the (XRD) peak appearing at the diffraction angle θ, (A) refers to the shape factor which its value depends on the crystalline shape (0.94). The micro strain was produced through growth of thin films and can be calculated from the following formula [18].

$$\delta = \frac{|a_{ASTM} - a_{XRD}|}{a_{ASTM}} \qquad (2)$$

Where (a) = the lattice constant and the internal levels spaces are calculated by using diffraction (Bragg) equation whereas n= a positive integer, d= the internal levels spaces [18].

$$n\,\lambda = 2\,d \sin\theta \qquad (3)$$

$$a = d \times (h^2 \times k^2 \times l^2)2 \qquad (4)$$

The Texture Coefficient (Tc) can be founded by applying the relationship [18]

$$T_{c\,(h,k,l)} = \frac{I\,(h,k,l)/I_{\circ}\,(h,k,l)}{N_r^{-1}\,\Sigma\, I(h,k,l)/\,I_{\circ}(h,k,l)} \qquad (5)$$

Where I = the measured intensity و Io= Intensity adopted in the cards (ASTM), Nr = the number of reflections. H, k, l = Miller coefficients. The film number of layers deposition on substrate can be calculated from the ratio between the thickness of the film and the average particle size [18].

$$N_l = \frac{t}{G.s} \qquad (6)$$

Where t = thickness and G.s = average grain size.

3. Results and Discussion

3.1. XRD Analysis

The X-ray diffraction (XRD) patterns of deposited cadmium oxide CdO films normally at (θ=0˚) and obliquely (θ=50˚ and θ=70˚), then oxides at temprture (773) K for (1:5) hour are shown in Figure (1), It clear in normal deposition the presence two peaks in the XRD patterns reveals that all the films are the polycrystalline cubic structure of CdO films while become sharp and single crystal in an oblique deposition at (θ=50˚ and 70˚) due to the columnar growth in the direction of evaporation source or perpendicular to the plane of substrate Furthermore, it is evident from all images that XRD, in both normal and oblique orientation, exhibits strong, sharp peaks at a diffraction angle (2θ) of (33) that correspond to the (111) planes (preferred orientation). Other studies have also confirmed similar behaviour [18]. As the incidence angle increases (0 to 70), the preferred orientation (111) plane's intensity increases as well as. These findings are consistent with previous research [19, 20]. Furthermore, we find that in the normal deposition (0˚) depicted in Figure (1), a minor peak attributed to the (200) reflections is present at 2θ = (38°). This reflection is absent in oblique deposition (50º and 70º) depicted in Figures (2 and 3), respectively. The conventional data for the cubic CdO crystal structure matches these peaks quite well. [(File No. 05-0640, 27, 19553) JCPDF] [22, 21]. The number of layers (Nℓ) and grain size (G.s) as a function of deposition angle were determined from the X-ray diffraction patterns; the micro-strain (δ%) and another parameter of the cadmium oxide CdO films were also estimated and presented in table (1), which calculated by use pervious equations. The chart makes it evident that, for all deposition angles, the preferred orientation's lattice constant value (111) is smaller than that of the ASTM cubic CdO, aº = cº = 4.695 Å). The FWHM indicates the presence of dislocations in the material [23]. It is equal to the width of the line profile (in degrees) at half of the maximum intensity [24]. Many of a polycrystalline material's qualities are strongly influenced by the size of its grains; the most well-known of these is the increase in strength and hardness that coincides with a decrease in grain size. This may be explained by the increase in crystallites from 70º shows above.

Table (1): Shows X-ray parameters for CdO thin films prepared at different angle and at temperature 773K for time1:5 hour.

ST (K)	θd (deg)	2θ (deg)	hkl	FWHM (deg)	d_{ASTM} (A˚)	d_{XRD} (A˚)	Δd (A˚)	$α_{XRD}$	G.s (nm)	Tc	N_L	δ %
773	0˚	33.257	111	0.1742	2.7000	2.6917	0.0083	4.662	49.71	1.6	12	0.57
		38.518	200	0.1763	2.3400	2.3353	0.0047	4.670	49.85	0.4	12	0.39
	50˚	33.307	111	0.1947	2.7000	2.6878	0.0122	4.655	44.48	1	13	0.71
	70˚	33.371	111	0.1506	2.7000	2.6828	0.0172	4.646	57.51	1	10	0.90

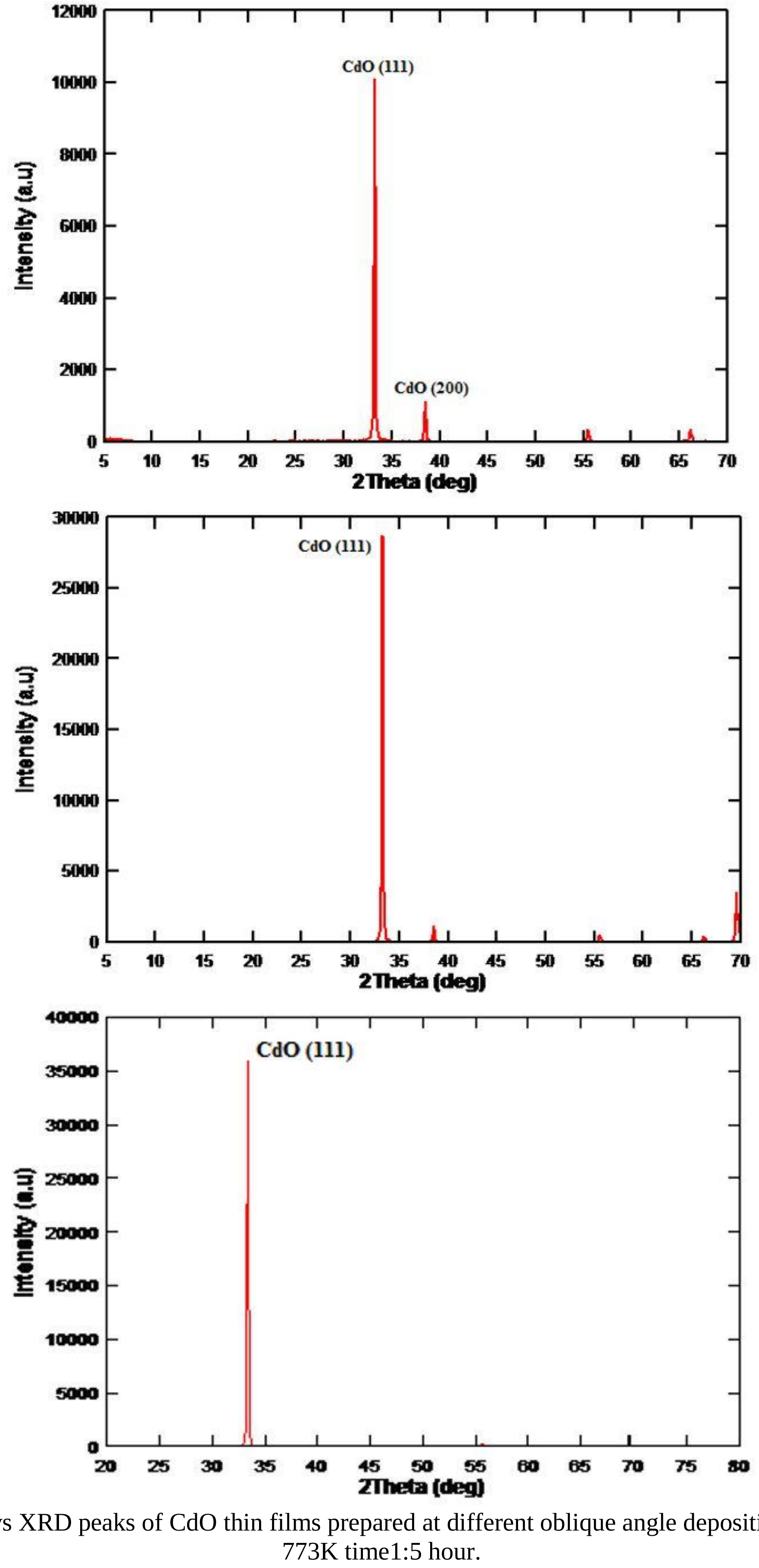

Figure (1): Shows XRD peaks of CdO thin films prepared at different oblique angle deposition at temperature 773K time1:5 hour.

3.2. Electrical Measurement

3.2.1. I-V Characteristics in Dark Conditions

The electrical behaviour of (Al/n-CdO/p-Si/Al) heterojunctions is generally determined depending on the properties of current-voltage characteristic curves. These properties represent the most important electrical characteristics that are used to describe heterojunction acts since all heterojunctions depend on these characteristics. Figure (4) shows the current density (J-V) characteristics under dark (The photodetectors were located in the black box to satisfy the darkness condition) in forward and reverse bias voltage of the normal and oblique (Al/CdO/p-Si/Al) photodetector. It can be noticed that the dark current for both normal and oblique angle (Al/CdO/p-Si/Al) heterojunction devices in the forward bias have two regions .The recombination process can occur when the produced carrier concentration (n*p > ni2), or when the carrier concentration is greater than the intrinsic carrier concentration (ni), as shown by the first low voltage, which is the recombination current. The diffusion current is represented by the second, which is at a high voltage. Additionally, there are two zones with reverse bias: The first occurs when the applied voltage is slightly increased in reverse current, which tends to produce electron-hole pairs at low bias. There is a noticeable rise in the reverse bias in the second section. In this instance, the current results from the diffusion of the minority carrier across the junction. Also, it is clear that the dark current increased linearity with applied voltage and decreased with increasing deposition angle at the fixed applied voltage. This is attributed to the columnar structure in the film, which in turn leads to an increase in the sheet resistance with increasing angle [25]. This also may be due to anisotropic columnar growing, which leads to homogeneity in electrical properties, especially for larger angles when the voids between columns come to be larger [26].

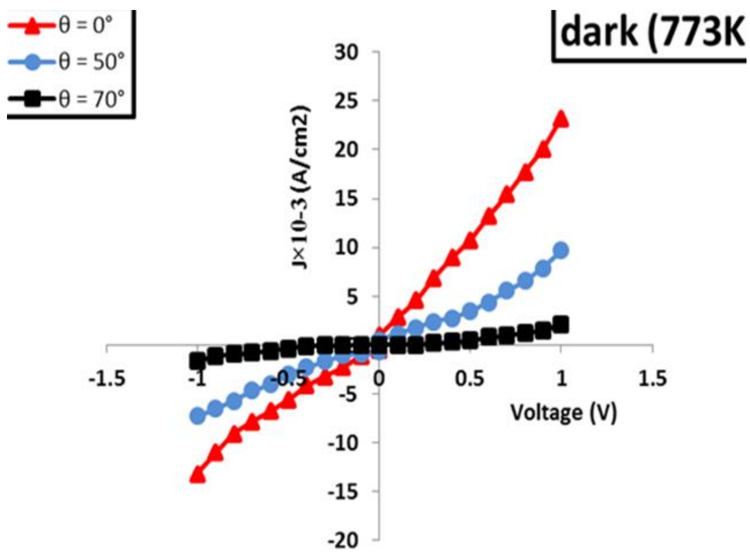

Figure (2): I-V characters in dark under forward and reverse bias for normal and oblique angle deposition (Al/CdO/p-Si/Al) photo detector prepared at 773K oxidation temperatures.

3.2.2. IV Characteristics under Illumination

Figure (3) shows the current density–voltage (J–V) characteristics for the normal θ= (0˚) and oblique θ= (50˚ and 70 ˚ (Al/CdO/p-Si/Al) heterojunctions that are prepared at oxidation temperature 773 K under light illumination situation (J-V measurements of photodetectors at reverse bias under illumination are carried out using 100W halogen lamp). The light illumination increases the reverse heterojunction photocurrent (the increasing width of the depletion layer under revere voltage bias), increases the absorbed photons number and the generated (e-h) pairs) and this increases with light intensity increasing also, this may be due to the diode decreasing resistance with illumination. From the figure below can be seen, that the photocurrent at a given voltage for the oblique (Al/CdO/p-Si/Al) heterojunction under illumination is higher than compared with the normal detector. The increase in charge production (I_{ph}) depends on the surface morphology of oblique CdO obviously, there is no saturation in photocurrent with light intensity increasing giving good linearity characteristics for fabricated photodetectors.

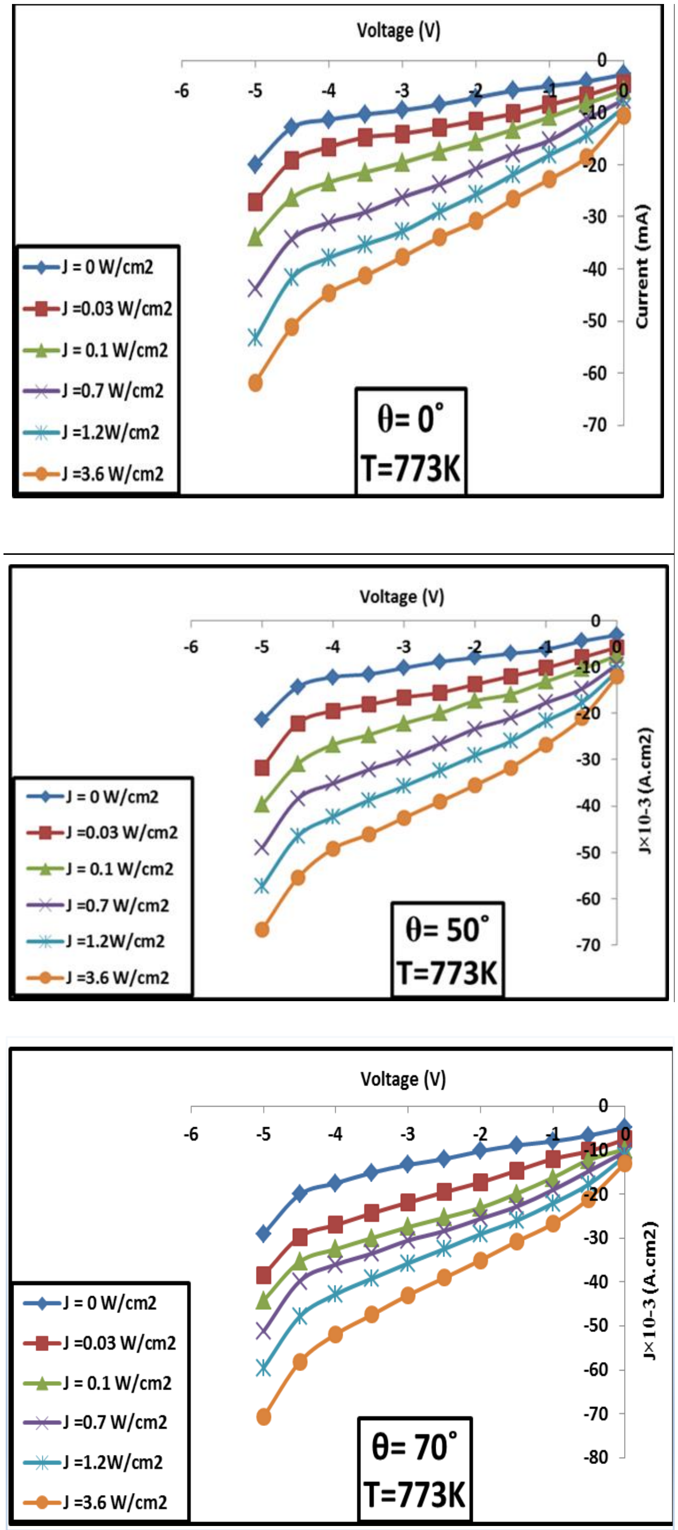

Figure (3): I-V characters in dark under forward and reverse bias for normal and oblique deposition (Al/CdO/p-Si/Al) photodetector prepared at oxidation temperature 773K.

3.3. Thermoelectric Power (Seebeck Effect)

Efficient solid-state energy conversion based on the thermoelectric (TE) effects, i.e., the Peltier effect for cooling and the Seebeck effect for power generation, has great potential in many applications. A high-performance TE material requires a high Seebeck coefficient (S), a high electrical conductivity σ, and a low thermal conductivity k, and its TE quality is described by the figure of merit (Z_T). Identifying or designing materials with a high (Z_T)

has proved to be extremely challenging in the past decades A theoretic and systematic study of the relationship between atomic structural features and TE properties will enhance the understanding of the transport mechanism in TE materials. This is very useful for the search and design of high-performance thermoelectric [27, 28]. The figure-of-merit of a thermoelectric material can be defined as [28]:

$$(ZT = s^2\sigma / k_{th}) \qquad (7)$$

Where (S) is the material's Seebeck coefficient ($V.K^{-1}$), (σ) is the material electrical conductivity ($\Omega.cm^{-1}$), (T) is the temperature (K) and K_{th} is the material thermal conductivity ($W.m^{-1}.K^{-1}$).

The thermal conductivity values for the polycrystalline CdO film are (0.682, 0.668, 0.632 W/cm.K) at temperatures (273,298 and 373) K respectively [29]. The electrical conductivity as a function of deposition angle was already measured, hence, determining the Seebeck coefficient is needed as a function of deposition angle, and this can be completed by measuring the potential difference developing at the two faces when making different temperatures between these two faces. Figure (6) shows the voltage difference (ΔV) depending on the CdO film temperature difference (ΔT) as a function of the deposition angle and the oxidation temperature. Analyzing the curves demonstrates all curves are almost linear, and the voltage difference value increased with increasing temperature difference and these increases are with both increasing deposition angle. This is due to the increase in electrons' movement toward the cold face. This is attributed to the temperature gradient (dT/dx) which creates a gradient in potential (dV/dx) in the material [30, 31]. From the slope of the ($\Delta V/\Delta T$) measurements, the thermoelectric power (S) was calculated by using the equation $S= \Delta V/\Delta T$. The Seebeck coefficient was found to (-S) value inducting (n-type) conductivity of the film It is clear that the Seebeck coefficient has a small value at deposition angles (0º, 50º) then increases for oblique angles (70º) since the decreasing in grain size is accompanied by smother surface (normal incidence, $\theta^o = 0$) which means less material per unit area contribute to the voltage difference is developed at the two surfaces and also in conventional semiconductors or metals, increasing electrical conductivity decreases the Seebeck coefficient due to the three electronic density-of states dimensional nature [32]. As shown in Table (2). So as to evaluate the possible use of these cadmium oxide (CdO) nanomaterials for thermoelectric application, firstly it has to determine the figure values of merit or, thermoelectric power factor (P.F) which is defined as (S2σ), this is in case of the lack of thermal conductivity data [33]. The power factor is calculated from the measured electrical conductivity (σ) and Seebeck Coefficient (S) as a function of the deposition angle of CdO thin films, as shown in Table (2). It's clear the power factor (P.F) calculated from equation P.F = S2 × σ as a function of deposition angle in CdO thin films the figure of merit (ZT) increases as deposition angle increases, this result, shows an enhancement in the figure of merit with oblique deposition as compared with the normal deposition. This may be due to increasing the angle that led to increasing the roughness and in turn a reduction in thermal conductivity and an increase in the figure of merit.

Table (2): Thermoelectric parameters (Seebeck Coefficient, Power Factor, and Figure of merit as a function of deposition angles and oxidation temperature for CdO thin films.

Deposition angle (deg)	Temperatures (K)	Seebeck coefficient (V/K)	Power Factor $W/K^2.cm$	Figure of merit (ZT) $(K)^{-1}$
0°	773	6.9×10^{-5}	6.71×10^{-13}	2.87×10^{-9}
50°		7.1×10^{-5}	2.46×10^{-12}	1.05×10^{-8}
70°		8×10^{-5}	1.4×10^{-12}	6.01×10^{-9}

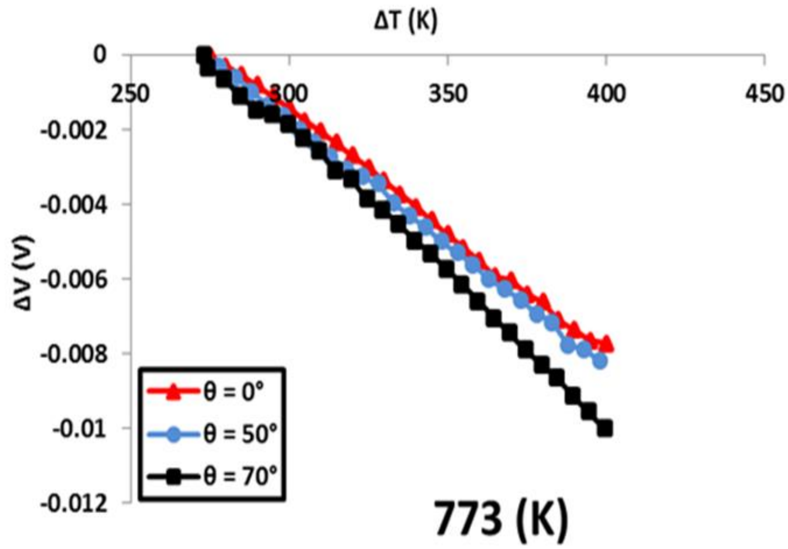

Figure (4): The voltage difference as a function of temperature difference for (CdO) thin films at different deposition angles (0˚, 50˚, and 70˚) at oxidation temperature 773 K.

4. Conclusions

Finally, we have discussed an experimental investigation of the oblique angle deposition method used to create CdO thin films. Further investigation reveals that the optoelectronic CdO heterojunction application is dependent on the oblique deposition angle for structural, thermoelectric, and electrical properties. The results of XRD studies indicate that all of the films have a preferential orientation along the (111) plane, and that intensity increases with increasing deposition angle. Additionally, the junction characteristics of the photodetectors are improved in oblique deposition (deposition angle 70^{o}) when compared to normal deposition.

Conflict of Interest: The authors declare that there are no conflicts of interest associated with this research project. We have no financial or personal relationships that could potentially bias our work or influence the interpretation of the results.

References

[1] P. A. Radi, A. G. Brito-Madurro, J. M. Madurro, and N. O. Dantas, “Characterization and properties of CdO nanocrystals incorporated in polyacrylamide,” *Brazilian Journal of Physics*, vol. 36, no. 2a, pp. 412–414, Jun. 2006, doi: 10.1590/s0103-97332006000300048.

[2] M. Al-Kinany, G. A. Al-Dahash, and J. Al-Shahban, “Effect of laser Fluence Energy on Morphological, Structural and Optical Properties of Gold and Silver Thin Films Prepared by Pulse Laser Deposition Method,” *Engineering and Technology Journal*, vol. 33, no. 9B, pp. 1561–1570, Nov. 2015, doi: 10.30684/etj.2015.117360.

[3] R. S. Mane, H. M. Pathan, C. D. Lokhande, and S.-H. Han, “An effective use of nanocrystalline CdO thin films in dye-sensitized solar cells,” *Solar Energy*, vol. 80, no. 2, pp. 185–190, Feb. 2006, doi: 10.1016/j.solener.2005.08.013.

[4] C. Danţuş, G. G. Rusu, M. Dobromir, and M. Rusu, “Preparation and characterization of CdO thin films obtained by thermal oxidation of evaporated Cd thin films,” *Applied Surface Science*, vol. 255, no. 5, pp. 2665–2670, Dec. 2008, doi: 10.1016/j.apsusc.2008.07.176.

[5] K. Senthil, Y. Tak, M. Seol, and K. Yong, “Synthesis and Characterization of ZnO Nanowire–CdO Composite Nanostructures,” *Nanoscale Research Letters*, vol. 4, no. 11, Jul. 2009, doi: 10.1007/s11671-009-9401-z.

[6] W. K. Khalef, E. K. Hamza, and A. A. Salman, “Morphology, Optical and Electrical Properties of Tin Oxide Thin Films Prepared by Spray Pyrolysis Method,” *Engineering and Technology Journal*, vol. 33, no. 3B, pp. 539–546, Mar. 2015, doi: 10.30684/etj.33.3b.13.

[7] P. Sakthivel, S. Asaithambi, M. Karuppaiah, S. Sheikfareed, R. Yuvakkumar, and G. Ravi, “Different rare earth (Sm, La, Nd) doped magnetron sputtered CdO thin films for optoelectronic applications,” *Journal of*

Materials Science: Materials in Electronics, vol. 30, no. 10, pp. 9999–10012, Apr. 2019, doi: 10.1007/s10854-019-01342-9.

[8] G. Anil Kumar, M. V. Ramana Reddy, and K. Narasimha Reddy, “Growth of highly transparent and conductive CdO thin films deposited at different thicknesses by RF reactive magnetron sputtering,” *Materials Research Innovations*, vol. 19, no. 3, pp. 204–211, Aug. 2014, doi: 10.1179/1433075x14y.0000000243.

[9] N. Raja, V. S. Nagarethinam, and A. R. Balu, “Aging effect of the precursor solution on the structural, morphological and opto-electrical properties of spray deposited CdO thin films,” *Materials Science-Poland*, vol. 37, no. 1, pp. 1–7, Mar. 2019, doi: 10.2478/msp-2019-0009.

[10] F. C. Eze, “Oxygen partial pressure dependence of the structural properties of CdO thin films deposited by a modified reactive vacuum evaporation process,” *Materials Chemistry and Physics*, vol. 89, no. 2–3, pp. 205–210, Feb. 2005, doi: 10.1016/j.matchemphys.2003.11.039.

[11] M. Aronniemi, J. Saino, and J. Lahtinen, “Characterization and gas-sensing behavior of an iron oxide thin film prepared by atomic layer deposition,” *Thin Solid Films*, vol. 516, no. 18, pp. 6110–6115, Jul. 2008, doi: 10.1016/j.tsf.2007.11.011.

[12] F. C. Eze, “Optical characterisation of thin film cadmium oxide prepared by a modified reactive thermal evaporation process,” *Global Journal of Pure and Applied Sciences*, vol. 9, no. 4, Apr. 2004, doi: 10.4314/gjpas.v9i4.16066.

[13] W. Cong, G. Wang, Q. Yang, J. Li, J. Hsieh, and R. Lai, “CT image reconstruction on a low dimensional manifold,” *Inverse Problems & Imaging*, vol. 13, no. 3, pp. 449–460, 2019, doi: 10.3934/ipi.2019022.

[14] M. M. Hawkeye and M. J. Brett, “Glancing angle deposition: Fabrication, properties, and applications of micro- and nanostructured thin films,” *Journal of Vacuum Science & Technology A: Vacuum, Surfaces, and Films*, vol. 25, no. 5, pp. 1317–1335, Jul. 2007, doi: 10.1116/1.2764082.

[15] K. Robbie, J. C. Sit, and M. J. Brett, “Advanced techniques for glancing angle deposition,” *Journal of Vacuum Science & Technology B: Microelectronics and Nanometer Structures Processing, Measurement, and Phenomena*, vol. 16, no. 3, pp. 1115–1122, May 1998, doi: 10.1116/1.590019.

[16] A. M .Mousaat.el "Study the Effect of Deposition Angle on Structural Properties of Zn thin films" Department of Applied Sciences, University of Technology issn: 18120380 pp. 666-690, 2012.v

[17] Abdolahzadeh Z. A. and Ghodsia F.E. "Optical and Structural Studies of SolGel Deposited Nanostructured CdO Thin Films: Annealing Effect" Acts Physical Polemical, Vol. 120, no. 3, 2011.

[18] W. K. Khalef, S. D.AL. ALgawi, and S. R. Mohammed, “Structure and Morphological Properties of Cadmium Oxide Nanostructure Prepared By Oblique Angle Deposition Method,” *Engineering and Technology Journal*, vol. 33, no. 9B, pp. 1741–1752, Nov. 2015, doi: 10.30684/etj.2015.117449.

[19] W. K. Khalef, “Preparation and Characterization of CdO Thin Films Obtained by Oxidation of Obliquely Evaporated Cd Thin Films,” *Journal of Al-Nahrain University Science*, vol. 17, no. 4, pp. 103–110, Dec. 2017, doi: 10.22401/jnus.17.4.14.

[20] H. R. A. Ali, “Effect of Substrate Temperature on Structural and Optical Properties of CdO Thin Films,” *International Letters of Chemistry, Physics and Astronomy*, vol. 27, pp. 47–55, Feb. 2014, doi: 10.56431/p-29712t.

[21] S. G. I. - and A. V. K. -, “Effect of Indium Doping on Structural Properties of Spray Pyrolysed Cadmium Oxide Thin Films,” *International Journal For Multidisciplinary Research*, vol. 5, no. 1, Jan. 2023, doi: 10.36948/ijfmr.2023.icmrs23.176.

[22] M. Aronniemi, J. Saino, and J. Lahtinen, “Characterization and gas-sensing behavior of an iron oxide thin film prepared by atomic layer deposition,” *Thin Solid Films*, vol. 516, no. 18, pp. 6110–6115, Jul. 2008, doi: 10.1016/j.tsf.2007.11.011.

[23] “Study of Composition and Morphology of Cadmium Oxide (CdO) Nanoparticles for Eliminating Cancer Cells,” *Journal of Nanomedicine Research*, vol. 2, no. 5, Dec. 2015, doi: 10.15406/jnmr.2015.02.00042.

[24] B. D. Cullity and R. Smoluchowski, “Elements of X-Ray Diffraction,” *Physics Today*, vol. 10, no. 3, pp. 50–50, Mar. 1957, doi: 10.1063/1.3060306.

[25] N. Hassan, “Fabrication of n-CdO NPs/PS Heterojunction by laser ablation in ethanol,” *Polytechnic Journal*, vol. 8, no. 2, pp. 299–308, Jun. 2018, doi: 10.25156/ptj.2018.8.2.165.

[26] K. Shimakawa, Meherun-Nessa, H. Ishida, and A. Ganjoo, “Quantum efficiency of light-induced defect creation in hydrogenated amorphous silicon and amorphous As2Se3,” *Philosophical Magazine*, vol. 84, no. 1, pp. 81–89, Jan. 2004, doi: 10.1080/14786430310001621490.

[27] A. A. Aljubouri, A. D. Faisal, and W. K. Khalef, "Fabrication of temperature sensor based on copper oxide nanowires grown on titanium coated glass substrate," *Materials Science-Poland*, vol. 36, no. 3, pp. 460–468, Sep. 2018, doi: 10.2478/msp-2018-0051.

[28] Kathleen C. Barron" Experimental Studies of the Thermoelectric Properties of Microstructured and Nanostructured Lead Salts" Febr [1]M. Lovett-Barron, "Sensory Neuroscience: Smelling Salts Lead Fish to Safety," *Current Biology*, vol. 31, no. 4, pp. R199–R201, Feb. 2021, doi: 10.1016/j.cub.2020.12.021.

[29] W. K. Khalef, A. A. Aljubouri, and A. D. Faisal, "Photo detector fabrication based ZnO nanostructure on silicon substrate," *Optical and Quantum Electronics*, vol. 52, no. 7, Jun. 2020, doi: 10.1007/s11082-020-02445-y.

[30] W. K.Khalef and W. Najeeb Ibrahim, "Study the Effect of Oblique Deposition on Surface Characterization and Microstructure of Evaporated Cadmium Thin Films," *Engineering and Technology Journal*, vol. 31, no. 2 B, pp. 130–141, Feb. 2013, doi: 10.30684/etj.31.2b.2.

[31] W. K. Khalef, "Preparation and Characterization of Teo2 Nan particles by Pulsed Laser Ablation in Water," *Engineering and Technology Journal*, vol. 32, no. 3B, pp. 396–405, Mar. 2014, doi: 10.30684/etj.32.3b.2.

[32] C. T. Lynch, *Handbook of Materials Science*. CRC Press, 2019.

[33] A. Thamer, A. Faisal, A. Abed, and W. Khalef, "Synthesis of gold-coated branched ZnO nanorods for gas sensor fabrication," *Journal of Nanoparticle Research*, vol. 22, no. 4, Mar. 2020, doi: 10.1007/s11051-020-04783-0.